

CANCELLATION EFFECT AND PARAMETER IDENTIFIABILITY OF SHIP STEERING DYNAMICS

by

Wei-Yuan Hwang*

Abstract

The identifiability problem of hydrodynamic coefficients in a nonlinear ship maneuvering model is presented. The contribution plot of hydrodynamic coefficients is analyzed to show the cancellation effect. Slender-body theory is applied to show that the cancellation effect is inherent for the steering dynamics of ships. Parameter transformation is introduced to overcome the difficulty in the coefficient estimation of linear terms. A practical approach is suggested to identify the nonlinear dynamics of ships.

Introduction

System identification is a sub-topic of estimation in the system theory. Based on a hypothesized structure, the parameters of the system are estimated by using the observations of system. If the resulting model passes the validity test, it is an equivalent of the real system, and the system is said identifiable in the sense that its input-output relationship can be verified and its behavior can be predicted. Furthermore, if the optimal parameter values can be estimated within the required accuracy of true values, the system is said parameter identifiable.

The system identification of ship maneuvering dynamics is attempted for several reasons. The identification of input-output relationship helps the evaluation of ship maneuverability, to build a realistic training simulator and the design of autopilot and navigation system. Moreover, if the maneuvering dynamics is parameter identifiable, the study of scale effect and ship-model correlation can be advanced by applying system identification techniques to both ship and its models.

Using the data of full scale experiment for identification, Åström & Källström (1976), Norrbin, Byström, Åström & Källström (1977), Byström & Källström (1978) and Hwang (1980) have shown that the ship maneuvering system is identifiable in the sense of input-output relationship. However, the estimation of hydrodynamic coefficients has not been satisfactory. In the following paragraphs, the discussion is mainly about the difficulties in identifying the hydrodynamic coefficients. Therefore, the derivation of ship maneuvering equations and the theory of system identification are omitted in this paper. However, the governing equations utilized by the author are provided in Appendix A for reference. The theory of system identification can be found in Schweppe (1973), Gelb (1974), Eykhoff (1974), Grauge (1976), Hsia (1979) and many others. The latest survey of its applications to ship motion will be found in the proceedings of 14th ITTC.

Simultaneous drifting phenomenon and cancellation effect

If a ship is performing moderate maneuvers in the calm sea, linearized governing equations are sufficient to describe the ship motion. Following the sign convention of Figure 1 and using the state variable expression, the equations have the following form,

$$\begin{bmatrix} m - Y_v & mx_G - Y_r \\ mx_G - N_v & I_z - N_r \end{bmatrix} \begin{bmatrix} \dot{v} \\ \dot{r} \end{bmatrix} = \begin{bmatrix} Y_v & Y_r - mu \\ N_v & N_r - mx_G u \end{bmatrix} \begin{bmatrix} v \\ r \end{bmatrix} + \begin{bmatrix} Y_\delta \\ N_\delta \end{bmatrix} \delta \quad (1)$$

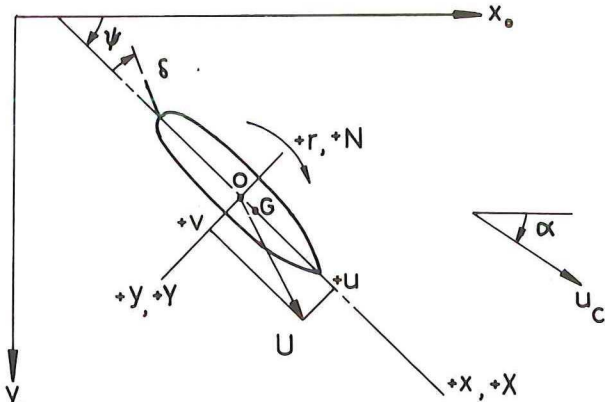


Figure 1. Coordinate system and sign convention.

Since the input-output relationship in (1) does not change by multiplying the equation with any non-singular matrix, it is impossible to estimate all the coefficients in (1) at the same time. For nonlinear models, the equations can not be written in the form of (1), but simultaneous estimation of all the coefficients is still not possible for the same reason. Fortunately, Fujino, Takashina & Yamamoto (1974) showed that finite element method can predict the added mass and added moment of inertia pretty accurately. Thus, the parameter identifiability problem of this attribute can be solved with the inertia coefficients being fixed on numerically determined values.

However, there is another problem of identifiability that has not been pointed out previously. A stochastic

^{a)} Institute of Naval Architecture, National Taiwan University, Taipei, Taiwan, Republic of China.

model based on Appendix A is used and the extended Kalman filtering is applied by the author to identify the ship steering dynamics. When N'_v , N'_r , Y'_v , Y'_r and other hydrodynamic coefficients were estimated simultaneously, a troublesome and yet interesting phenomenon occurred. At certain point during the estimation, coefficients N'_v and N'_r started to drift together in a similar pattern. Nevertheless, the measurements of state variables were filtered very well. Figure 2 is an illustration of this simultaneous drifting phenomenon that occurs specifically when the extended Kalman filtering is applied to do the estimation. In which the simulated $10^\circ/10^\circ$ zigzag maneuvering data of ESSO OSAKA, see Appendix B for its principal dimensions

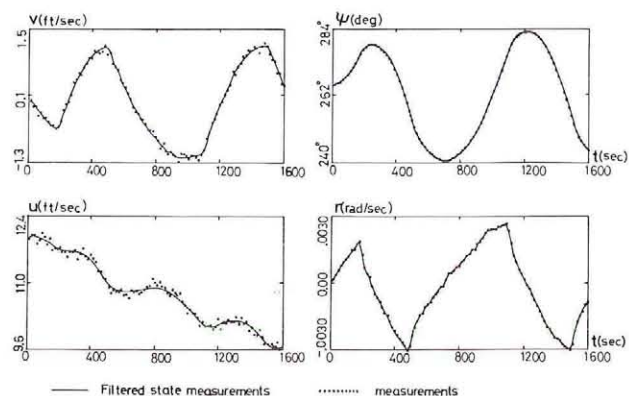


Figure 2a. Results of identification to illustrate the phenomenon of 'simultaneous drift'. The filtering of simulated measurements of ESSO OSAKA for a $10^\circ/10^\circ$ zigzag maneuver.

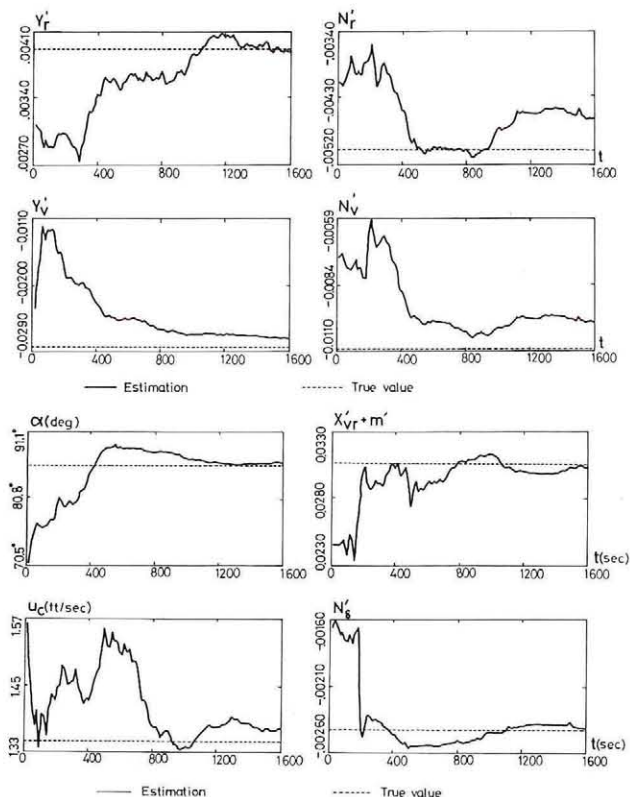


Figure 2b. The estimation of hydrodynamic coefficients and current from the simulated maneuvering data in Figure 2a.

Table 1

Estimated hydrodynamic coefficient from the simulated $10^\circ/10^\circ$ zigzag test data of ESSO OSAKA and the true value of these coefficients used for generating the simulated data

	initial estimate	estimated	true value
u_c (ft/sec)	1.620	1.373	1.350
α (deg)	68.800	86.368	86.000
Y'_v	-0.02262	-0.02719	-0.02828
Y'_r	0.00312	0.00387	0.00391
N'_v	-0.00872	-0.00984	-0.01090
N'_r	-0.00400	-0.00458	-0.00500
N'_δ	-0.00194	-0.00241	-0.00242
$X'_{vr} + m'$	0.02456	0.03044	0.03070

and characteristics, was processed to estimate the hydrodynamic coefficients Y'_v , Y'_r , N'_v , N'_r , N'_δ , $X'_{vr} + m'$, current magnitude u_c and direction α . The results of estimation are summarized in Table 1. Notice that if Y'_v and $Y'_r - m'u'$ are estimated together, simultaneous drift also occurs, although the simultaneous estimation of Y'_v and Y'_r does not have this problem. The simultaneous drifting phenomenon implies that the value of N'_v and N'_r can be simultaneously increased or decreased according to certain implicit rules and the mathematical model still generates the same ship motion response to the identical rudder execution. In other words, there is a nonuniqueness problem of the estimated parameter values, i.e., the problem of parameter identifiability.

In the study by Norrbin, Åström, Byström and Källström (1977), the maximum likelihood method (MLM) was applied and a nonlinear model was used to process the zigzag maneuvering data collected from experiments at sea. The results are reproduced in Tables 2, 3, 4 for reference. Due to the different nature between the MLM and the method of extended Kal-

Table 2

Estimated hydrodynamic derivatives from a $20^\circ/20^\circ$ zigzag test with the USS COMPASS ISLAND. A nonlinear model is used. (Norrbin, et al. (1977), Byström and Källström (1978))

	initial estimate	MLM	output error
Y''_{uv}	-1.454	-1.863	-3.201
$Y''_{ur} - 1$	-0.659	-1.096	-1.588
N''_{uv}	-0.365	-0.154	-0.089
$N''_{ur} - x''_G$	-0.231	-0.078	-0.053
Y''_δ	0.348	0.223	0.193
N''_δ	0.167	-0.107	-0.093

Table 3

Estimated hydrodynamic derivatives from a $10^\circ/10^\circ$ zig-zag test with the SEA SCAPE. A nonlinear model is used. (Norbinn, et al. (1977))

	initial estimate	MLM
Y''_{uv}	-0.700	-0.988
$Y''_{ur} - 1$	-0.820	-0.700
N''_{uv}	-0.350	1.082
$N''_{ur} - x''_G$	-0.163	-0.527
Y''_δ	0.176	0.378
N''_δ	-0.083	-0.178

Table 4

Estimated hydrodynamic derivatives from a $10^\circ/10^\circ$ zigzag test with the A K FERNSTROM. A nonlinear model is used. (Norbin, et al. (1977), Byström and Källström (1978))

	initial estimate	MLM	output error
Y''_{uv}	-1.200	-0.817	-0.831
$Y''_{ur} - 1$	-0.750	-0.673	-0.715
N''_{uv}	-0.450	-0.227	-0.239
$N''_{ur} - x''_G$	-0.230	-0.111	-0.124
Y''_δ	0.230	0.227	0.237
N''_δ	-0.108	-0.107	-0.111

man filtering, the MLM does not generate the figure similar to Figure 2. Therefore, the simultaneous drifting phenomenon can not occur when the MLM is applied to identify the hydrodynamic coefficients. However, its results of estimation indicate that the estimated hydrodynamic coefficients can be substantially different from the adjusted value of model test, and yet the identified system can simulate the ship steering dynamics satisfactorily. Using another technique, the output error method, Byström & Källström (1978) processed the same set of data and similar situations also resulted. The estimated coefficient values are included in Tables 2 and 4 for comparison. The problem of parameter identifiability not only occurs in the study of ship steering dynamics but also occurs in the study of the other modes of motion, e.g., Sandman & Kelly (1974) have identified a positive damping coefficient M_q of pitching motion for an underwater vehicle. Since different estimation techniques have been applied and different ships were analyzed to identify the ship steering dynamic system, the common symptoms of parameter identifiability should have an explanation.

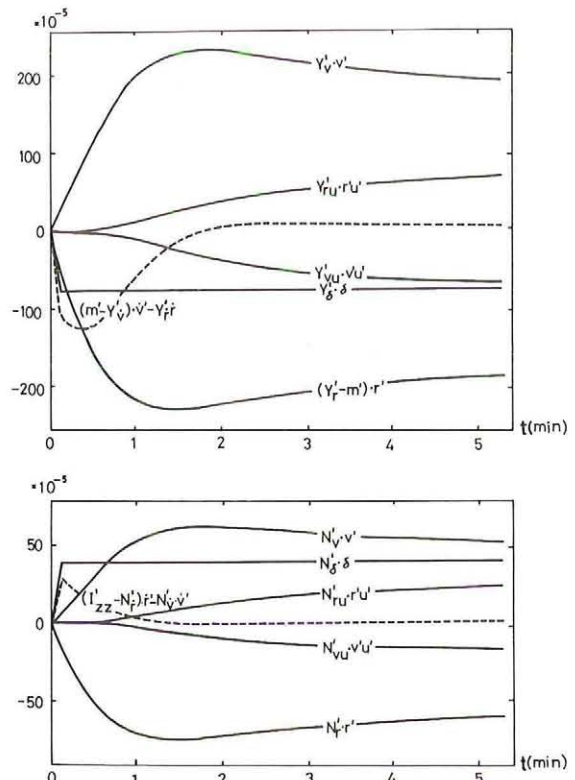


Figure 3. Time histories of separate terms of force and moment equation during a 19° rudder turning circle, rpm = 100, $u_0 = 8\text{m/sec}$. (Ref. Leeuwen (1972)).

In a study of ship maneuverability, Leeuwen (1972) investigated the force and moment component contributed by each hydrodynamic coefficient to the ship motions. He showed that during a simulated turning maneuver of BRITISH BOMBARDIA, see Figure 3, the time history of $Y'_v v'$ and that of $(Y'_r - m')r'$ not only possess the same pattern but also have the similar order of magnitude, except that the sign is opposite. The same situation also occurs to $N'_v v'$ and $N'_r r'$. Since in Figure 3 the same resultant Y force can be obtained by adjusting Y'_v and $Y'_r - m'$ simultaneously at equal percentages and the same resultant N moment can be obtained by adjusting N'_v and N'_r simultaneously at equal rate, it explains why turning maneuver is not suitable for the estimation of hydrodynamic coefficients. Apparently, the cancellation effect had caused the simultaneous drifting problems that occurred to Lundblad (1974), when simulated data of turning maneuvers was processed to estimate the linear hydrodynamic coefficients. Nevertheless, the simultaneous drifting phenomenon also happened when zigzag maneuvering data was processed, as shown in Figure 2. It is suspected that the cancellation effect is not a consequence of constant rudder deflection, instead, it is more likely an intrinsic nature of the ship dynamic system.

To confirm this speculation, an investigation similar to Figure 3 was carried out to study the contribution

of each hydrodynamic coefficient to the $10^\circ/10^\circ$ zigzag, the $20^\circ/20^\circ$ zigzag and the biased zigzag maneuvers. These simulations for ESSO OSAKA employed the model-test value of hydrodynamic coefficient and the sea-trial record of rudder execution. The results are presented in Figures 4 to 6. Surprisingly, there is no

discrepancy of the cancellation effect between the maneuvers of constant rudder deflection and the maneuvers of continuous rudder execution. This finding accounts for the simultaneous drift of N'_v and N'_r and the simultaneous drift of Y'_v and $Y'_r - m'u'$.

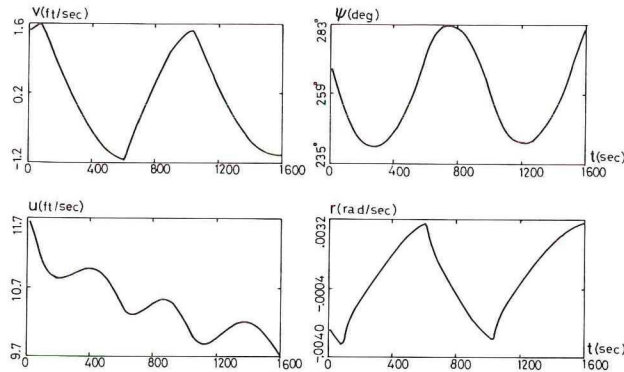


Figure 4a. Simulated $10^\circ/10^\circ$ zigzag maneuver for ESSO OSAKA at rpm = 41.4.

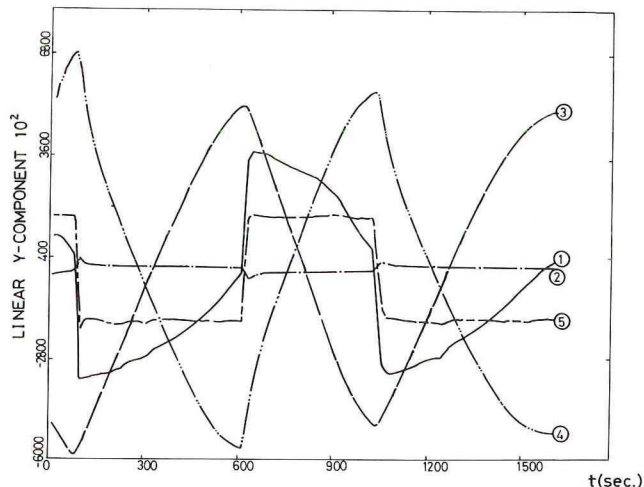


Figure 4b. Time histories of linear Y-terms in the force equation of Appendix A, during the simulated maneuver in Figure 4a. Curve notations are defined in Table 5.

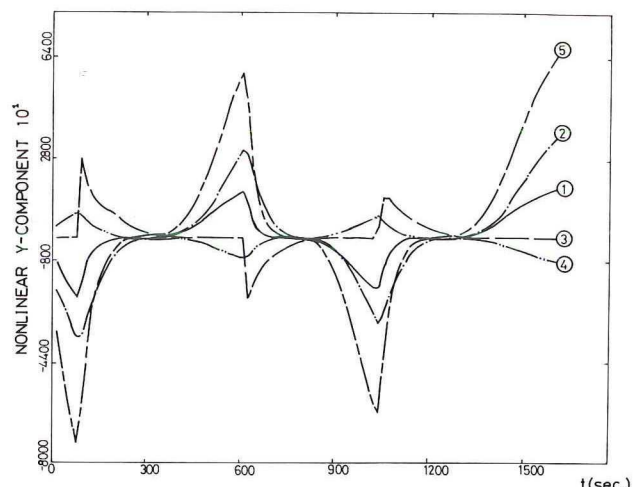


Figure 4c. Time histories of nonlinear Y-terms in the force equation of Appendix A, during the simulated maneuver in Figure 4a. Curve notations are defined in Table 5.

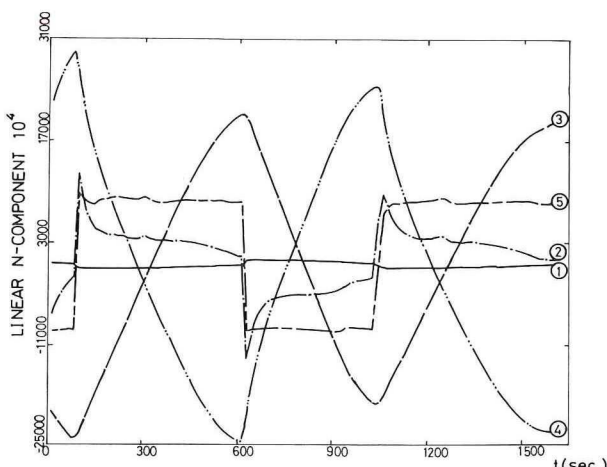


Figure 4d. Time histories of linear N-terms in the moment equation of Appendix A, during the simulated maneuver in Figure 4a. Curve notations are defined in Table 5.

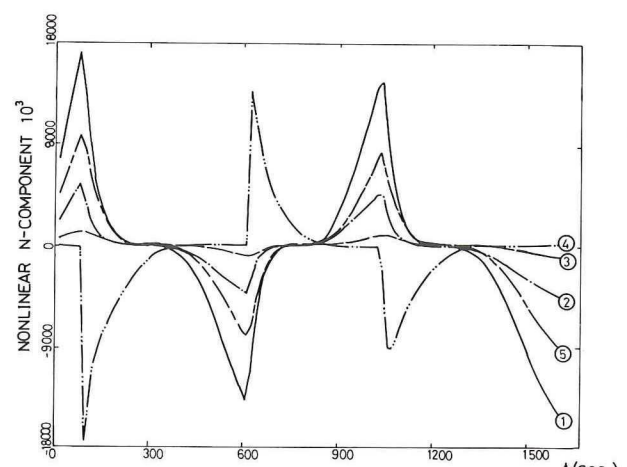


Figure 4e. Time histories of nonlinear N-terms in the moment equation of Appendix A, during the simulated maneuver in Figure 4a. Curve notations are defined in Table 5.

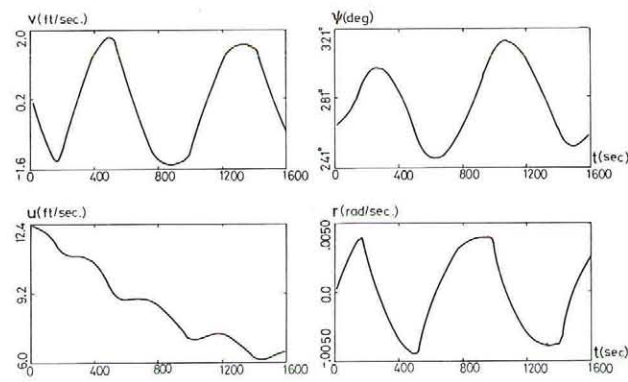


Figure 5a. Simulated $20^\circ/20^\circ$ zigzag maneuver for ESSO OSAKA at rpm = 40.5.

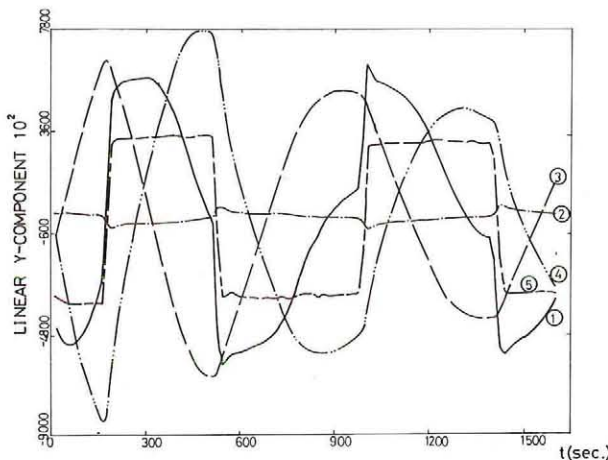


Figure 5 b. Time histories of linear Y-terms in the force equation of Appendix A, during the simulated maneuver in Figure 5a. Curve notations are defined in Table 5.

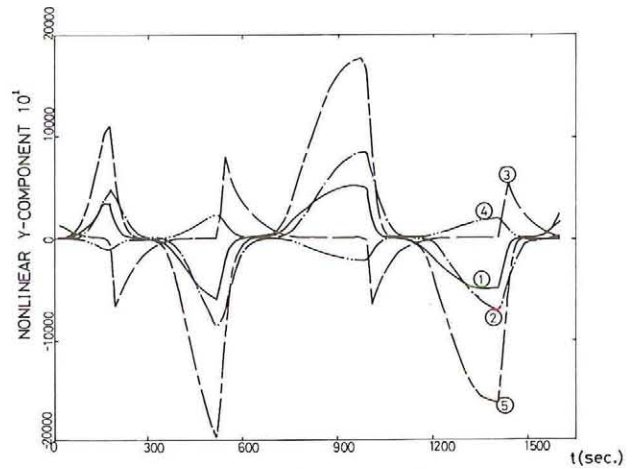


Figure 5c. Time histories of nonlinear Y-terms in the force equation of Appendix A, during the simulated maneuver in Figure 5a. Curve notations are defined in Table 5.

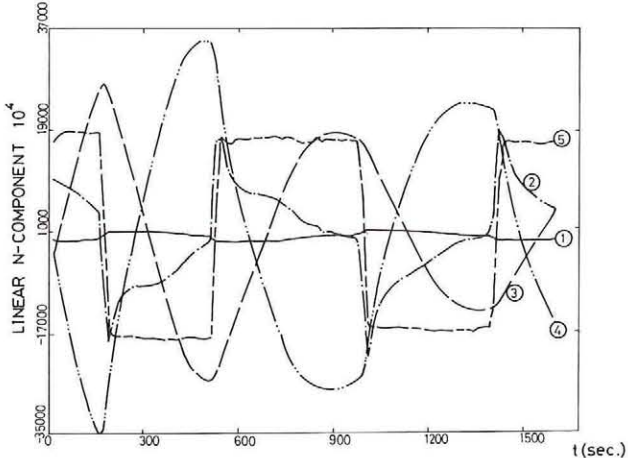


Figure 5d. Time histories of linear N-terms in the moment equation of Appendix A, during the simulated maneuver in Figure 5a. Curve notations are defined in Table 5.

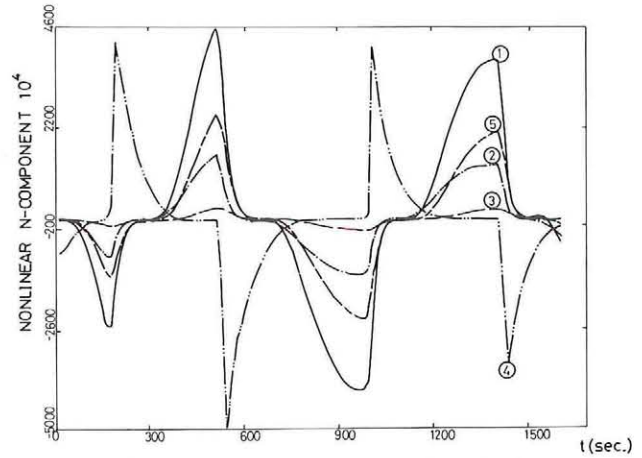


Figure 5e. Time histories of nonlinear N-terms in the moment equation of Appendix A, during the simulated maneuver in Figure 5a. Curve notations are defined in Table 5.

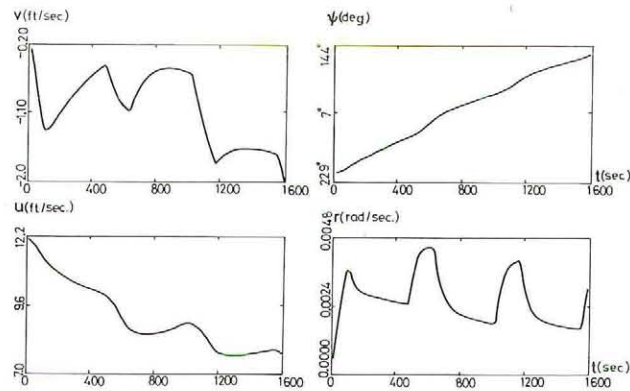


Figure 6a. Simulated biased zigzag ($15^\circ \pm 10^\circ$) maneuver for ESSO OSAKA at rpm = 40.4.

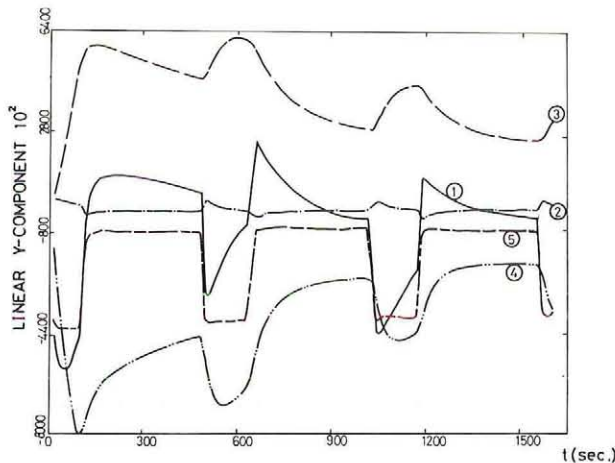


Figure 6b. Time histories of linear Y-terms in the force equation of Appendix A, during the simulated maneuver in Figure 6a. Curve notations are defined in Table 5.

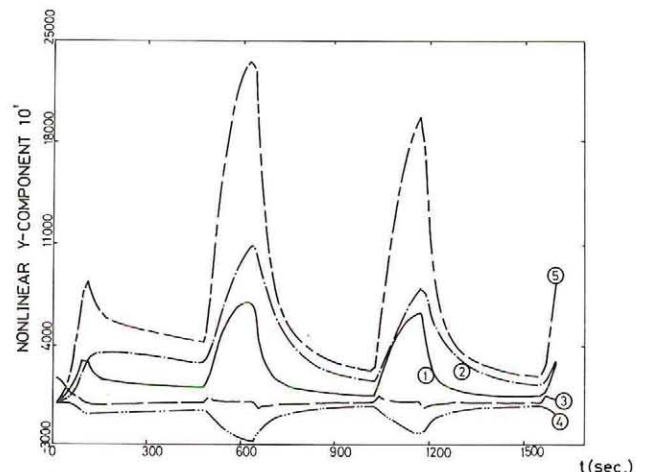


Figure 6c. Time histories of nonlinear Y-terms in the force equation of Appendix A, during the simulated maneuver in Figure 6a. Curve notations are defined in Table 5.

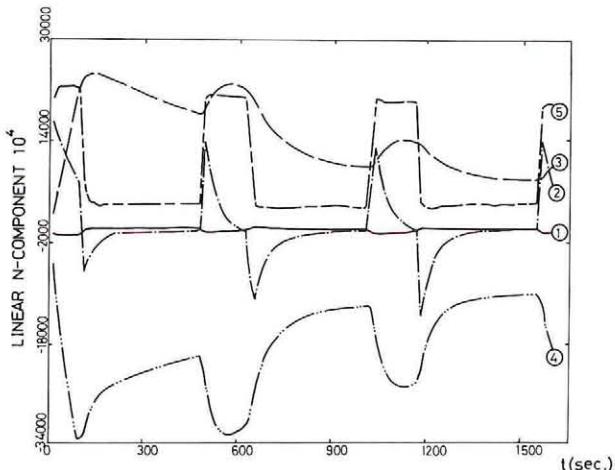


Figure 6d. Time histories of linear N-terms in the moment equation of Appendix A, during the simulated maneuver in Figure 6a. Curve notations are defined in Table 5.

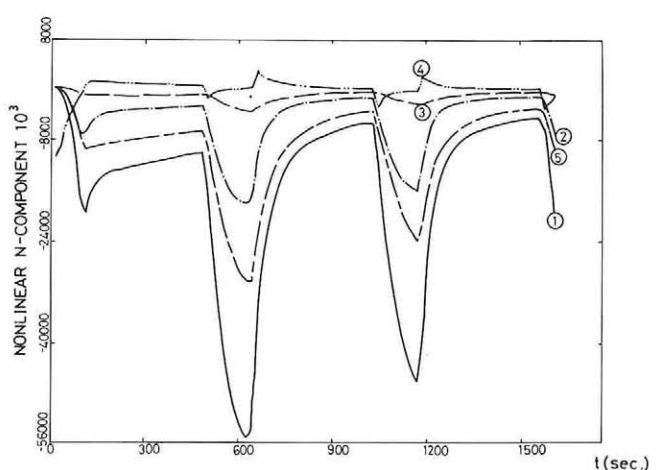


Figure 6e. Time histories of nonlinear N-terms in the moment equation of Appendix A, during the simulated maneuver in Figure 6a. Curve notations are defined in Table 5.

Theoretical analysis

Now that the cancellation effect causes the simultaneous drift, it is necessary to understand why the force and moment contributions of hydrodynamic coefficients tend to cancel with each other. Here, the slender-body theory is applied to study this problem. In order to simplify the analysis, it is assumed that the maneuver is mild and no current as well as other environmental influences exist. Following the sign convention of Figure 1 and the derivation of Newman (1977), the hydrodynamic sway force and yaw moment upon a maneuvering ship are expressed as in the following equations,

$$Y = -\dot{v}m_{22}^s + \dot{r}m_{26}^s - uv m_{22}(x_T) - ur x_T m_{22}(x_T) \\ + m_{22}(x_T) u^2 \delta \quad (2)$$

$$N = -\dot{v}m_{26}^s + \dot{r}m_{66}^s + uv[m_{22}^s + x_T m_{22}(x_T)] \\ + ur[m_{26}^s - x_T^2 m_{22}(x_T)] + m_{22}(x_T) u^2 \delta x_T \quad (3)$$

$$m_{22}^s = \int_L m_{22}(x) dx \quad (4)$$

$$m_{66}^s = \int_L m_{22}(x) x^2 dx \quad (5)$$

$$m_{26}^s = -\int_L m_{22}(x) x dx \quad (6)$$

where

$m_{22}(x)$ is the two dimensional added mass in y -direction,

δ is the rudder deflection,

x_T is the value of x at the effective trailing edge, and

the superscript 's' denotes strip theory.

Equating these hydrodynamic force and moment to the inertia force and moment, the following equations of motion are obtained,

$$uv m_{22}(x_T) + u[x_T m_{22}(x_T) + m] r \\ + (m_{22}^s + m) \dot{v} - (m_{26}^s + M_{26}) \dot{r} \quad (7)$$

$$= m_{22}(x_T) u^2 \delta$$

$$-uv[m_{22}^s + x_T m_{22}(x_T)] + u[m_{26}^s + M_{26} - x_T^2 m_{22}(x_T)] r \\ + (m_{26}^s + M_{26}) \dot{v} - (m_{66}^s + M_{66}) \dot{r} = m_{22}(x_T) u^2 \delta x_T \quad (8)$$

where M_{66} is the moment of inertia about z axis. In order to simplify the problem, the slender body is assumed of circular cross section and constant draft T , except that it has a point bow and a tail fin. Also it is assumed that the origin is located at midship and the ship mass is of the same magnitude as the sway added mass m_{22}^s , which is a fairly realistic approximation for the real ship configurations. Thus,

$$m_{22}(x) = \frac{\rho}{2} \pi T^2$$

$$m_{26}^s + M_{26} = 0 \quad (9)$$

$$x_T = -0.5 L$$

According to (7), (8) and (9),

$$Y_v v + (Y_r - mu)r = [-um_{22}(x_T)] v \\ + [-ux_T m_{22}(x_T) - mu] r \quad (10)$$

$$N_v v + (N_r - mx_G u)r = [um_{22}^s + ux_T m_{22}(x_T)] v \\ + [ux_T^2 m_{22}(x_T)] r \quad (11)$$

If $Y_v v$ cancels $(Y_r - mu)r$ completely and $N_v v$ cancels $(N_r - mx_G u)r$ completely, both (10) and (11) requires that

$$v + 0.5 rL = 0 \quad (12)$$

Since pivot point is defined as

$$x_p \equiv -\frac{v}{r}, \quad (13)$$

Therefore, if the pivot point is located at the bow of this slender body, $Y_v v$ and $(Y_r - mu)r$ or $N_v v$ and $(N_r - mx_G u)r$ will cancel each other entirely. In other words, in this special case, the inertia forces and moments are completely balanced by rudder force and moment. Since this case is over-simplified, its conclusion can not be applied to real ships. However, it has been found that $Y_v v$ cancels $(Y_r - mu)r$ and $N_v v$ cancels $(N_r - mx_G u)r$ to a large extent for the real ship, thus the pivot point is hypothesized to be near the bow. In Figure 7, the positions of pivot point during the simulated maneuvers in Figures 4, 5 and 6 are plotted against time. It is emphasized that the sway velocity relative to current is used to calculate the pivot position. Figure 8 is a plot of the pivot position of BRITISH BOMBARDIER during the turning maneuver in Figure 3. Since these plots of the instantaneous position of pivot point do justify the previous hypothesis, therefore, as long as the pivot point is near the bow, $Y_v v$ cancels $(Y_r - mu)r$ and $N_v v$ cancels $(N_r - mx_G u)r$ to a large extent.

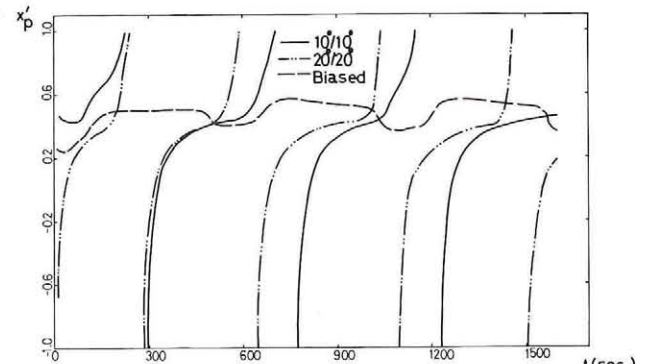


Figure 7. Time history of the positions of pivot point during the simulated maneuvers in Figure 4, 5 and 6.

Table 5
Definitions of curve notations for Figures 4, 5 and 6

Y	linear	nonlinear
— ① $(m - Y_v) \dot{v}$		$Y'_{r^3} (\frac{\rho}{2} L^5 U_r^{-1}) r^3$
— · — ② $(mx_G - Y_r) \dot{r}$		$Y'_{v_r^3} (\frac{\rho}{2} L^2 U_r^{-1}) v_r^3$
— — ③ $Y'_{v_r} (\frac{\rho}{2} L^2 U_r) v_r + Y'_\delta (c - c_o) \frac{\rho}{2} L^2 v_r$		$Y'_{e^3} (\frac{\rho}{2} L^2 c^2) e^3$
— .. — ④ $(Y'_r - m'u'_r) (\frac{\rho}{2} L^3 U_r) r - \frac{Y'_\delta}{2} (c - c_o) \frac{\rho}{2} L^3 r$	$\frac{Y'_\delta}{2} (c - c_o) \frac{\rho}{2} L^3 r$	$Y'_{v_r^2 r} (\frac{\rho}{2} L^3 U_r^{-1}) v_r^2 r$
— - - ⑤ $Y'_\delta (\frac{\rho}{2} L^2 c^2) \delta$		$Y'_{r^2 v_r} (\frac{\rho}{2} L^4 U_r^{-1}) r^2 v_r$

N	linear	nonlinear
— ① $(mx_G - N_v) \dot{v}$		$N'_{r^2 v_r} (\frac{\rho}{2} L^5 U_r^{-1}) r^2 v_r$
— · — ② $(I_z - N_r) \dot{r}$		$N'_{r^3} (\frac{\rho}{2} L^6 U_r^{-1}) r^3$
— — ③ $N'_{v_r} (\frac{\rho}{2} L^3 U_r) v_r - N'_\delta (c - c_o) \frac{\rho}{2} L^3 v_r$		$N'_{v_r^3} (\frac{\rho}{2} L^3 U_r^{-1}) v_r^3$
— .. — ④ $(N'_r - m'x'_G u'_r) (\frac{\rho}{2} L^4 U_r) r + \frac{1}{2} N'_\delta (c - c_o) \frac{\rho}{2} L^4 r$	$\frac{1}{2} N'_\delta (c - c_o) \frac{\rho}{2} L^4 r$	$N'_{e^3} (\frac{\rho}{2} L^3 c^2) e^3$
— - - ⑤ $N'_\delta (\frac{\rho}{2} L^3 c^2) \delta$		$N'_{v_r^2 r} (\frac{\rho}{2} L^4 U_r^{-1}) v_r^2 r$

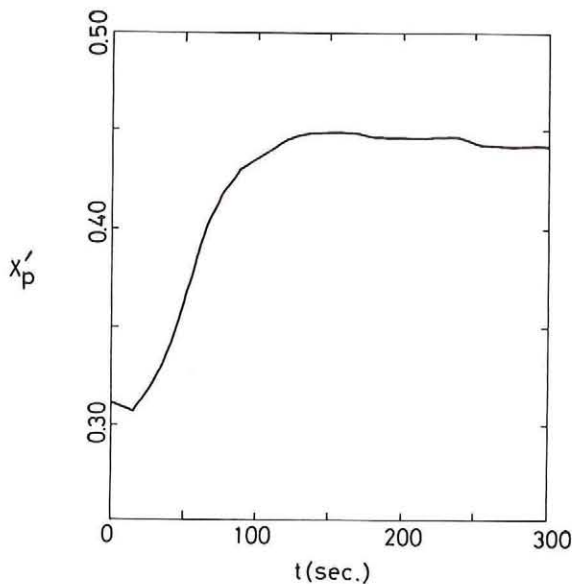


Figure 8. Time history of the pivot position of BRITISH BOMBARDIER during the turning maneuver in Figure 3.

Examine Figure 4 to 8 closely, there is something worth noticing. The singular behavior of pivot position at the beginning of a turning maneuver or during the progress of a zigzag maneuver shows that although the pivot position is near the bow during most of the time of maneuver, it is not defined when the yaw speed approaches zero. From the view point of kine-

matics, the ship motion is close to pure sway at that moment, thus the instantaneous turning center is located at infinity. In extreme condition, if the ship moves at constant heading, the propeller induced sway force Y_0 is balanced by $Y_v v$ and $Y_\delta \delta$ only and the yaw moment N_0 is balanced by $N_v v$ and $N_\delta \delta$ only. Since cancellation effect does not exist and the turning center is located at infinity steadily, it is deduced that the cancellation effect is weak when the singular behavior of pivot point occurs during any maneuver. Examining Figure 4 to 8, one can find that the statement is justified.

Cancellation effect and identifiability of non-linear coefficients

The estimation of nonlinear hydrodynamic coefficients is more difficult than that of the linear coefficients. This is not only because of the estimation error of the linear terms can exceed the contributions of nonlinear terms, but also because of the cancellation effect occurs to the nonlinear hydrodynamic coefficients too. Since the yaw speed has similar patterns to those of the sway speed, except that the sign is opposite, the contribution of each nonlinear coefficient is also similar to each other's in pattern. Consequently, it is very difficult to identify their values.

In Figures 4, 5 and 6, it is clear that the contributions of Y'_{vvv} , Y'_{rrr} , etc. can compensate each other or can be adjusted simultaneously at the same percentage to result in the same resultant nonlinear Y-force. Figure 9 is the sample estimation of nonlinear coefficients for ESSO OSAKA by processing the simulated maneuvering data.

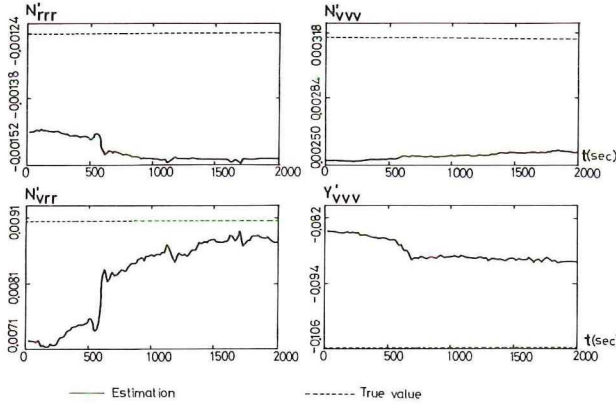


Figure 9. Results of identification. Biased zigzag maneuvering data of ESSO OSAKA (simulated) is processed to estimate the nonlinear coefficients.

Parameter transformation

From the experience of processing the simulated data, it has been realized that the percentage variance of N'_v and N'_r is always very close when ‘simultaneous drift’ occurs. In other words, if N'_v is 15% less than the true value, then N'_r is also 15% less than the true value. Similar situation applies to Y'_v and $Y'_r - m'u'$, but not to Y'_v and Y'_r . Based on these observations, two parameters, μ_Y and μ_N are introduced into the model of ship motion,

$$\mu_Y \equiv \frac{Y'_r - m'u'}{Y'_v} \quad (14)$$

$$\mu_N \equiv \frac{N'_r - m'x'_G u'}{N'_v} \quad (15)$$

Thus,

$$Y'_v \left(\frac{\rho}{2} L^2 U \right) v + (Y'_r - m'u') \left(\frac{\rho}{2} L^3 U \right) r \\ = Y'_v \left(\frac{\rho}{2} L^2 U \right) (v + \mu_Y Lr) \quad (16)$$

$$N'_v \left(\frac{\rho}{2} L^3 U \right) v + (N'_r - m'x'_G u') \left(\frac{\rho}{2} L^4 U \right) r \\ = N'_v \left(\frac{\rho}{2} L^3 U \right) (v + \mu_N Lr) \quad (17)$$

Since these transformations convert the linear expressions (in terms of the hydrodynamic coefficient) into nonlinear expressions, the likelihood surface around the true coefficient value is not a horizontal ridge with respect to Y'_v and μ_Y as well as with respect

to N'_v and μ_N any more. The new set of coefficient is more identifiable than the original set. Figure 10 shows the result of estimation that the parameter transformation technique is applied to estimate the coefficient value from simulated measurement of ESSO OSAKA. The second pass of estimation, which takes the estimated values of first pass at the initial guesses, is run to ascertain that the ‘simultaneous drift’ does not happen. Since the estimations are very successful, parameter transformation is proved an effective scheme to overcome the difficulty of estimation due to cancellation effect.

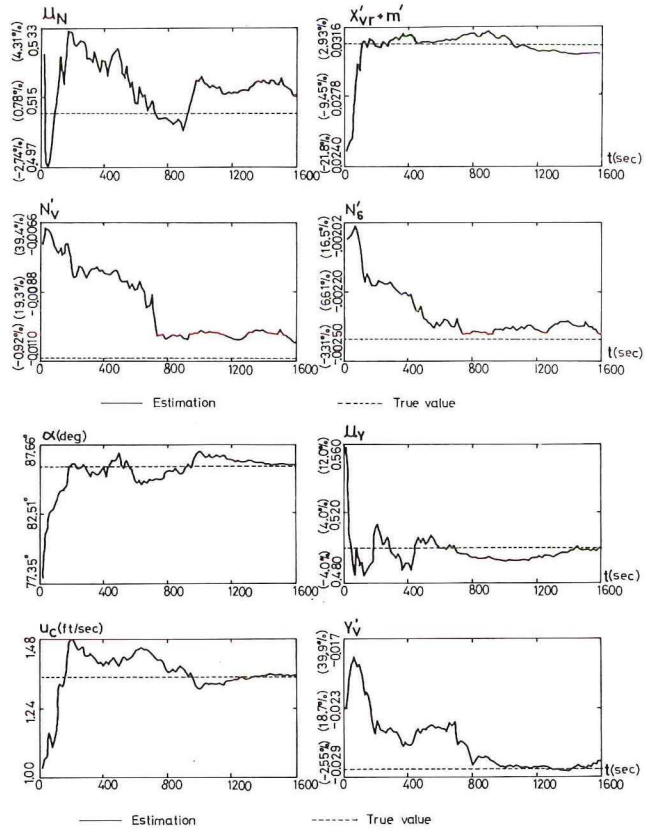


Figure 10a. Results of identification. Parameter transformation is applied to estimate the coefficients from the simulated maneuvering data of ESSO OSAKA.

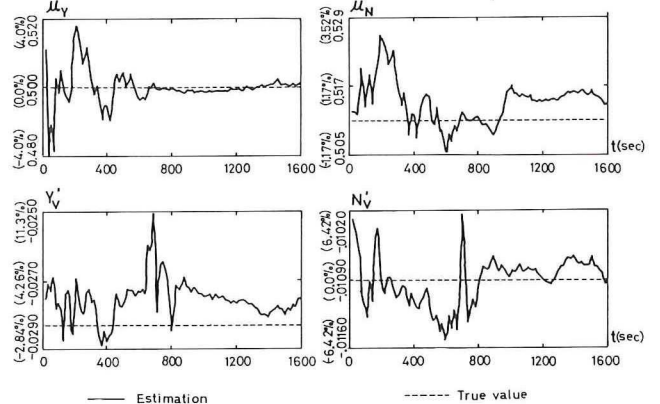


Figure 10b. Results of identification, second pass of the parameter estimation. The estimated coefficient value of Figure 10a is used as initial guess.

Nevertheless, the parameter transformation can not be applied to the estimation of nonlinear coefficients. Because when more than one nonlinear force coefficients are transformed, the μ'_Y 's can still compensate each other to give an equivalent nonlinear force contribution. And the situation for nonlinear moment coefficients is also the same. Consequently, if all, but one, of the $v-r$ cross related nonlinear coefficients are fixed at the model testing value, the adjustment of that nonfixed coefficient will absorb the errors of the rest of $v-r$ cross related coefficients. According to this argument, the nonlinear portion of the ship dynamics is identifiable only in the sense of input-output relationship, and the attempt on nonlinear-coefficient identification is practically impossible. For example, Y'_{eee} , Y'_{vrr} , N'_{eee} and N'_{vrr} is one of the many combinations of nonlinear coefficients, that the estimation of their value from the system measurements can give the optimal representation of nonlinear behavior in Y and N . Notice that, the contributions of Y'_{eee} is different from those of the other nonlinear Y coefficients and the contributions of N'_{eee} is different from those of the other nonlinear N coefficients. Therefore, having Y'_{eee} and N'_{eee} estimated is always necessary during the identification of nonlinear effect.

Although not mentioned in the previous discussion, the identification of nonlinear X coefficients has similar difficulty and the same strategy as in the identification of nonlinear Y -force and N -moment should be adopted.

Concluding remarks.

The simultaneous drift phenomena, when the extended Kalman filtering is applied to estimate the coefficient values, is found caused by the cancellation of the coefficients' contributions to the hydrodynamic forces and moments. The cancellation effect is an intrinsic nature of the dynamics of ship motion and no maneuver is discriminated. The slender-body theory is applied to show this nature.

When the simulated data is processed, the true value of coefficients and the estimated coefficient values of simultaneous drift give almost the same log likelihood. Therefore, the estimated coefficient values of simultaneous drift is mathematically acceptable, although they may not be feasible in the physical sense. The parameter transformation scheme is an effective method to eliminate the simultaneous drift phenomena. It has been successful when the simulated data was tested.

Since the sway speed is always similar in pattern with the yaw speed, the $v-r$ cross correlated nonlinear coefficients can compensate each other to give the same nonlinear effect. Therefore, to estimate all

the nonlinear coefficients simultaneously would be impossible. A set of nonlinear coefficients should be chosen to be estimated to give an equivalent nonlinear effect of the true system.

Acknowledgement

The content of this paper is part of the dissertation that has been accomplished in M.I.T. under the supervision of Professor M.A. Abkowitz. The author would like to express great gratitude to him. Many helpful suggestions have come from Professor R.W. Yeung and are sincerely appreciated. The author is grateful to his wife, Shau-Ley Hsi, who has done the typing of manuscript and the inking work of the computer graphical output. The support by the MARAD is also acknowledged.

Nomenclature

A_R	rudder area
A_p	rudder area of the portion that is in the slip stream
C_R	resistance coefficient
c	mean speed over the rudder
c_o	mean speed over the rudder of equilibrium propeller loading at forward speed u
d	propeller diameter
e	effective rudder angle
k	ratio of u_A to $u_{A\infty}$
L	characteristic length, length between perpendicular in this study
m	mass of ship
m_{ij}	added mass for $i, j = 1, 2, 3$ and added moment of inertia for $i, j = 4, 5, 6$
N	hydrodynamic moment in z -direction
N_0	asymmetrical yaw moment due to a single propeller
n	propeller rotating speed
r	yaw speed
S	wetted surface area
U	resultant ship speed
u_0	forward speed at equilibrium state
u	forward speed during maneuvers
u_A	propeller induced velocity
$u_{A\infty}$	propeller induced velocity far down stream
u_c	current speed
v	sway speed
w	wake fraction
X	hydrodynamic force in x -direction
x_G	position of the center of gravity
x_p	position of pivot point
Y	hydrodynamic force in y -direction
Y_0	asymmetrical sway force due to single propeller
α	current direction

- δ rudder angle
 μ_Y Y -force parameter introduced in the scheme of parameter transformation
 μ_N N -moment parameter introduced in the scheme of parameter transformation
 ρ water density
 ψ heading angle

Superscript

- ' indicates nondimensionalized quantities
 $^\circ$ degree
 $^.$ $\frac{d}{dt}$
 s indicates quantities calculated by strip theory

Subscript

- r indicates speed relative to water

References

- Åström, K.J. and Källström, C.G., 1976, 'Identification of ship steering dynamics', *Automatica*, Vol. 12, pp. 9–22.
- Åström, K.J., and Källström, C.G., 1973, 'Application of system identification techniques to the determination of ship dynamics', *Proceedings 3rd IFAC Symposium on Identification and System Parameter Estimation*, The Hague, The Netherlands.
- Byström, L. and Källström, C.G., 1978, 'System identification of linear and non-linear ship steering dynamics', *Proceedings 5th Ship Control System Symposium*, Washington, D.C.
- Eykoff, P., 1974, 'System identification', Wiley, London.
- Fujino, M., Takashina, J., and Yamamoto, S., 1974, 'On the three-dimensional correction factors for the added mass and the added mass moment of inertia related to maneuverability in shallow water', *Journal Society Naval Architects*, Vol 135, Japan.
- Gelb, A., ed., 1974, 'Applied optimal estimation', The M.I.T. Press, Cambridge, MA.
- Grauge, D., 1976, 'Identification of systems', Krieger Publishing Co., Inc.
- Lundblad, J.G., 1974, 'Application of the extended Kalman filtering technique to ship maneuvering analysis', M.I.T. Master Thesis, Department of Ocean Engineering.
- Newman, J.N., 1977, 'Marine hydrodynamics', The M.I.T. Press, Cambridge, MA.
- Norbin, N.H., Åström, K.J., Byström, L. and Källström, C.G., 1977, 'Further studies of parameter identification of linear and non-linear ship steering dynamics', Report 1920–6, Swedish State Shipbuilding Experiment Tank, Gothenburg, Sweden.
- Sandman, B.E. and Kelly, J.C., 1974, 'System identification: Application to underwater vehicle dynamics', *J. Hydraulics*, Vol. 8, No. 3, pp. 94–99.
- Schwepple, F.C., 1973, 'Uncertain dynamic systems', Prentice Hall, Inc.
- Leeuwen, G. van, 1972, 'Prediction of ship maneuverability', Netherlands Ship Research Center TNO, Report No. 1583.
- Hwang, W.Y., 1980, 'Application of system identification to ship maneuvering', M.I.T. Ph.D. Thesis, Department of Ocean Engineering.
- Smitt, L.W. and Chislett, M.S., 1974, 'Large amplitude PMM tests and maneuvering predictions for a Mariner Class vessel', *Tenth Symposium on Naval Hydrodynamics*.
- Abkowitz, M.A., 1969, 'Stability and motion control of ocean vehicles', The M.I.T. Press, Cambridge, MA.

Appendix A**Governing equations of ship steering dynamics**

To describe the ship motion in horizontal plane, Newton's law of motion is applied. In the coordinate system of Figure 1. The following differential equations are obtained for the case of no current appearance,

$$\begin{aligned} m(\dot{u} - rv - x_G r^2) &= X \\ m(\dot{v} + ru + x_G \dot{r}) &= Y \\ I_z \dot{r} + mx_G (\dot{v} + ru) &= N \end{aligned} \quad (A.1)$$

where X , Y , N are functions of ship properties, fluid properties, motion properties and orientations. If there is a steady current u_c in the direction of α , then the relative motions of ship to water are

$$\begin{aligned} u_r &= u - u_c \cos(\psi - \alpha) \\ v_r &= v + u_c \sin(\psi - \alpha) \\ \dot{u}_r &= \dot{u} + u_c r \sin(\psi - \alpha) \\ \dot{v}_r &= \dot{v} + u_c r \cos(\psi - \alpha) \end{aligned} \quad (A.2)$$

Substituting (A.2) into (A.1), it is found that

$$\begin{aligned} m(\dot{u}_r - rv_r - x_G r^2) &= X(\dot{u}_r, \dot{v}_r, \dot{r}, u_r, v_r, r, \delta, \dots) \\ m(\dot{v}_r + ru_r + x_G \dot{r}) &= Y(\dot{u}_r, \dot{v}_r, \dot{r}, u_r, v_r, r, \delta, \dots) \\ I_z \dot{r} + mx_G (\dot{v}_r + ru_r) &= N(\dot{u}_r, \dot{v}_r, \dot{r}, u_r, v_r, r, \delta, \dots) \end{aligned} \quad (A.3)$$

Due to the complex nature of fluid flow around ship hull, a closed form expression of the hydrodynamic forces and moments is almost impossible. Therefore, the hydrodynamic force and moment are expressed in terms of the Taylor expansion with respect to the motion variables and the deflection of control surface about an equilibrium point, at which $u_r = u_{0r}$, $v_r = r = \dot{u}_r = \dot{v}_r = \dot{r} = \delta = 0$. In order to include the nonlinear effect and yet to keep the number of terms low, the terms of order higher than 3 are considered small and thus are neglected. The resulting equations are similar to those obtained by Abkowitz (1969). However, they are not feasible for the purpose of system identification. The lack of physical significance and the difficulty of measurement of many nonlinear terms are the major reasons. The validity test of system identification also indicates the modelling problem when the sea-trial data is utilized by the author, such as data-

file dependence and non-white normalized residuals. Based on the experience of processing the sea trial data, the following modifications are made to give a better modelling of ship steering dynamics:

- Instead of the ship speed, the averaged flow speed over rudder is employed as the dimensional parameter for the rudder induced forces and moments.
- $X_u \Delta u + X_{uu} (\Delta u)^2 + X_{uuu} (\Delta u)^3$ is replaced by $\eta_1 u^2 + \eta_2 u n + \eta_3 n^2 - \frac{\rho}{2} C_R u^2 S$ in order to make the expression independent of the equilibrium point, about which the Taylor series is expanded.
- The effect of unequilibrium propeller loading on the linear coefficient, Y'_v , Y'_r , N'_v and N'_r , is modelled by modifying the original coefficient with an extra term in terms of Y'_δ or N'_δ , instead of using the lengthy series expansion in terms of $Y'_{v_r \mu_r}$, $Y'_{ru_r \mu_r}$, $Y'_{v_r \mu_r \mu_r}$, $N'_{v_r \mu_r}$, $N'_{ru_r \mu_r}$, $N'_{v_r \mu_r \mu_r}$, $N'_{ru_r \mu_r}$ and so on.
- The ship forward speed u is replaced by the propeller induced speed at propeller, i.e. $0.5 u_{A_\infty}$ as the speed parameter for the unbalanced force Y'_0 and moment N'_0 owing to the odd number of propeller.
- The nonlinear forces and moments arising from the cross coupling of v , r and δ is replaced by a simple expression in terms of the effective rudder angle e .
- Since a small error in $X'_{vr} + m'$ can induce a significant effect on the surge speed u , and the estimated values of $X'_{vr} + m'$ varies significantly from the mild maneuvers to the violent maneuvers, $X'_{v_r 2r 2}$ is introduced to account for this phenomenon. A better modification is still being sought for.

After these modifications, the governing equations of ship motion have the following form:

$$\begin{aligned}\dot{u} &= \dot{u}_r - u_c \cdot r \cdot \sin(\psi - \alpha) \\ \dot{u}_r &= \frac{f_1}{m - X_{u_r}} \\ \dot{v} &= \dot{v}_r - u_c \cdot r \cdot \cos(\psi - \alpha) \\ \dot{v}_r &= \frac{1}{f_4} [(J_z - N_r) f_2 - (mx_G - Y_r) f_3] \\ \dot{r} &= \frac{1}{f_4} [(m - Y_{v_r}) f_3 - (mx_G - N_{v_r}) f_2]\end{aligned}\quad (A.4)$$

$$\dot{\psi} = r$$

where

$$\begin{aligned}f_1 &= \eta'_1 [\frac{\rho}{2} L^2] u_r^2 + \eta'_2 [\frac{\rho}{2} L^3] n u_r + \eta'_3 [\frac{\rho}{2} L^4] n^2 \\ &\quad - C_R [\frac{\rho}{2} S u_r^2] + X'_{v_r 2} [\frac{\rho}{2} L^2] v_r^2 + X'_{e 2} [\frac{\rho}{2} L^2 c^2] e^2 \\ &\quad + (X'_{r 2} + m' x_G) [\frac{\rho}{2} L^4] r^2 + (X'_{v_r r} + m') [\frac{\rho}{2} L^3] v_r r\end{aligned}$$

$$\begin{aligned}f_2 &= Y'_0 [\frac{\rho}{2} L^2 (\frac{u_{A_\infty}}{2})^2] + \{Y'_v [\frac{\rho}{2} L^2 U_r] v_r \\ &\quad + Y'_\delta (c - c_0) \frac{\rho}{2} L^2 v_r\} + \{(Y'_r - m' u_r) [\frac{\rho}{2} L^3 U_r] r \\ &\quad - \frac{Y'_\delta}{2} (c - c_0) \frac{\rho}{2} L^3 r\} + Y'_\delta [\frac{\rho}{2} L^2 c^2] \delta \\ &\quad + Y'_{v_r 3} [\frac{\rho}{2} L^2 U_r^{-1}] v_r^3 + Y'_{v_r 2r} [\frac{\rho}{2} L^3 U_r^{-1}] v_r^2 r \\ &\quad + Y'_{r 2v_r} [\frac{\rho}{2} L^4 U_r^{-1}] r^2 v_r + Y'_{r 3} [\frac{\rho}{2} L^5 U_r^{-1}] r^3 \\ &\quad + Y'_{e 3} [\frac{\rho}{2} L^2 c^2] e^3 \\ f_3 &= N'_0 [\frac{\rho}{2} L^3 (\frac{u_{A_\infty}}{2})^2] + \{N'_v [\frac{\rho}{2} L^3 U_r] v_r \\ &\quad - N'_\delta (c - c_0) \frac{\rho}{2} L^3 v_r\} + \{N'_r - m' x'_G u_r) [\frac{\rho}{2} L^4 U_r] r \\ &\quad + \frac{1}{2} N'_\delta (c - c_0) \frac{\rho}{2} L^4 r\} + N'_\delta [\frac{\rho}{2} L^3 c^2] \delta \\ &\quad + N'_{v_r 3} [\frac{\rho}{2} L^3 U_r^{-1}] v_r^3 + N'_{v_r 2r} [\frac{\rho}{2} L^4 U_r^{-1}] v_r^2 r \\ &\quad + N'_{r 2v_r} [\frac{\rho}{2} L^5 U_r^{-1}] r^2 v_r + N'_{r 3} [\frac{\rho}{2} L^6 U_r^{-1}] r^3 \\ &\quad + N'_{e 3} [\frac{\rho}{2} L^3 c^2] e^3 \\ f_4 &= (m' - Y'_{v_r}) [\frac{\rho}{2} L^3] (J_z - N_r) [\frac{\rho}{2} L^5] \\ &\quad - (m' x'_G - N'_{v_r}) [\frac{\rho}{2} L^4] (m' x'_G - Y'_r) [\frac{\rho}{2} L^4]\end{aligned}$$

$$u_r = u - u_c \cos(\psi - \alpha)$$

$$v_r = v + u_c \sin(\psi - \alpha)$$

$$c = \sqrt{\frac{A_p}{A_R} [(1-w) u_r + k u_{A_\infty}]^2 + \frac{A_R - A_p}{A_R} (1-w)^2 u_r^2}$$

(refer Figures A.1 and A.2)

$$U_r = \sqrt{u_r^2 + v_r^2}$$

$$e = \text{effective rudder angle} \approx \delta - \frac{v}{c} + \frac{rL}{2c}$$

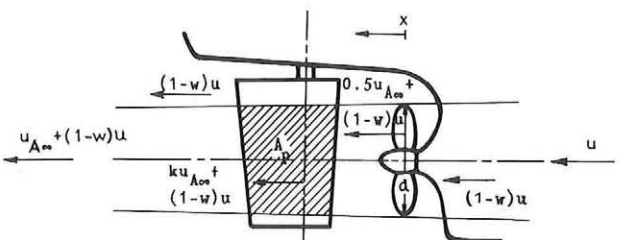


Figure A.1. Geometrical relationship between the propeller and the rudder. Propeller race is computed according to momentum theory.

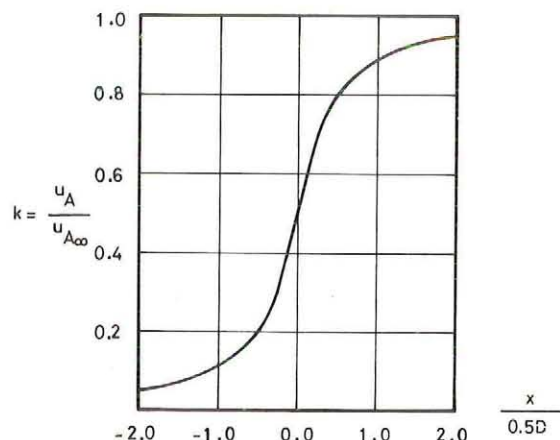


Figure A2. Mean axial velocity induced by a semi-infinite tube of ring vortices determined by the law of Biot-Savart (ref. Smitt & Chislett (1974)).

Appendix B

Main dimensions and characteristics of ESSO OSAKA and other ships

	ESSO OSAKA	BRITISH BOMBARDIER	USS COMPASS ISLAND	SEA SCAPE	A K FERNSTROM
Length LBP (m)	325.0	221.0	161.1	350.0	243.9
Beam (m)	53.0	29.6	23.2	60.0	38.9
Draught (m)	22.05	12.50	9.1	22.3	14.9
Displacement (m^3)	328,880	65,089	20,840	389,100	121,500
Number of blades	5	5	-	-	-